

Keldysh-Lattice Boltzmann approach to quantum nanofluidics

Sauro Succi *

*IIT Center for Life Nano-Neuroscience at La Sapienza,
Viale Regina Elena 291, 00161, Roma, Italy*

Andrea Montessori

*Roma Tre University, Department of Civil, Computer Science and Aeronautical Technologies Engineering, Rome,
00146, Italy*

We present a mathematical and computational framework to couple the Keldysh non equilibrium quantum transport formalism with a nanoscale lattice Boltzmann method for the computational design of quantum-engineered nanofluidic devices.

I. Introduction

The general trend of modern science and engineering towards miniaturization has placed a strong premium towards the study of fluid phenomena at nanometric scales. This tendency draws from many technological sources, aeronautics and aerospace, biomedical, chemical-pharmaceutical and energy/environment being just a few prominent ones. Given the vast amount of energy lost on frictional contacts, low friction is a paramount goal for the optimal design of most micro and nano-mechanical devices involved in these applications.

According to continuum mechanics, the pressure gradient to push a given mass flow across a channel of diameter D scales like D^{-4} , a relation that speaks clearly for the difficulty of pushing flows across miniaturized devices: a ten-fold decrease in radius demands a ten-thousand fold increase in the required pressure. The above scaling derives from the assumption that the fluid molecules in contact with solid walls do not exhibit any net motion, the so called *no-slip* condition, because they remain trapped in local corrugations of the solid wall. This assumption is no longer valid whenever the size of the channel becomes comparable with the molecular mean free path and, more generally, whenever the fluid-solid molecular interactions can no longer be described in terms of simple mechanical collisions. Whatever the driving mechanism, the onset of a non-zero fluid velocity at the wall (slip flow), $u_s \neq 0$, is a much-sought effect, as it turns the hydrodynamic D^{-4} barrier into a much more manageable D^{-2} dependence. Slip flow is typically quantified in terms of the so called slip length $L_s = u_s / (du/dy)_w$ where $(du/dy)_w$ is the velocity gradient at the wall. Under no-slip condition L_s is of the order of the molecular mean free path, i.e. about 1 nm for water, while suitably treated (geometrically or chemically) walls can reach up to $L_s \sim 10 \div 100$ nm, which is comparable to the size of the nano-device, leading to a very substantial decrease of the effective viscosity (roughly speaking a factor D/L_s). Achieving large slip lengths involves the nano-engineering of fluid-wall interactions such as to prevent fluid molecules from being mechanically trapped by nano-corrugations. This is usually pursued by clever geometrical and/or chemical coatings, so as to promote near-wall repulsion between fluid and solid molecules (hydrophobic coating).

However, in the recent years, it has been argued and experimentally shown that unanticipated quantum-electro-mechanical interfacial phenomena can lead to a major reduction of frictional losses [1, 2].

In this paper we wish to discuss prospects designing suitable computational solvers embedding ab-initio non-equilibrium quantum mechanical phenomena within a mesoscale computational harness, capable of exploring the effects of the aforementioned quantum transport phenomena at scales of experimental relevance.

We begin by discussing the basic physical scenario.

II. The physical set up

We consider a fluid of water molecules flowing in a nano-channel, say a carbon nanotube (CNT) confined by carbon walls, say graphite or graphene. The flow of liquid water is driven by an external pressure gradient and this energy supply is dissipated to the walls. However, at variance with the classical picture, whereby such dissipation would result from mechanical collisions of the water molecules with solid molecules at the wall, new interfacial couplings need to be taken into account. The first observation is that at these nanoscopic scales, the charge fluctuations of the water

*Senior Researcher, IIT Center for Life Nano-Neuroscience at La Sapienza, sauro.succi@gmail.com

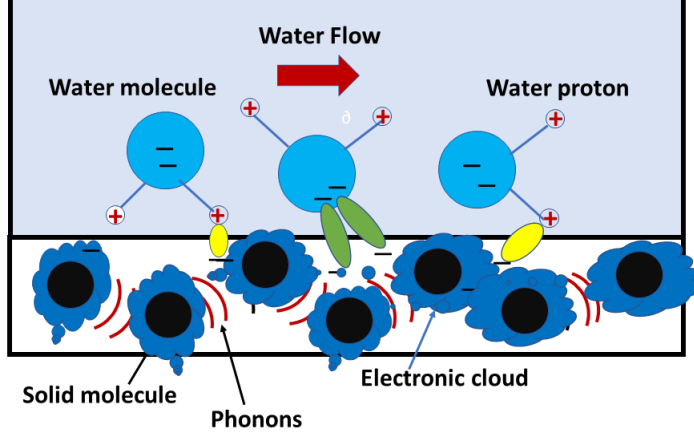


Fig. 1 The quantum friction scenario. The fluid part consists of water molecules (light blue full circles) subject to charge fluctuations (hydrons). The solid part consist of a crystal (full black circles), valence electrons and lattice vibrations (phonons). The ovals represent coupling between charge fluctuations and electronic degrees of freedom in the solid. Depending on the sign and orientation of the coupling, the hydrons in the liquid maybe dragged or accelerated, the latter instance resulting in drag reduction on the liquid water.

molecules at the liquid/solid interface couple with the electronic degrees of freedom in the solid, via screened Coulomb electrostatics. Given that De Broglie wavelength of electrons in metals is typically of the order of 10 nm , such coupling is indeed pretty plausible. The fluctuations of water molecules also couple to phonons excited by the direct impact of the water molecules on the solid wall. This generates a "phonon wind" in the solid which can in turn trigger a corresponding "electron wind" in the solid via electron-phonon scattering. Both species finally lose energy to the solid crystal, which acts as a ultimate energy sink.

A detailed analysis based on the quantum non-equilibrium Keldysh formalism, shows that the interaction between these three "species", hydrons (the charge fluctuations in the liquid), electrons in the solid and phonons also in the solid, leads to a rich variety of frictional exchanges between the flowing water and the electron/phonon "fluids" in the solid. Interestingly such exchanges can lead to a number of fascinating effects, such as a sizeable reduction of the effective friction experienced by the water liquid, the so called "negative quantum friction" effect, and also "electronic current drive", namely a net flow of electrons in the solid triggered by quantum interfacial effects.

Remarkably, the Keldysh analysis provides an analytical expression of these frictional effects in terms of classical-looking Langevin terms of the form $\gamma_{kl}(u_k - u_l)$ where $k, l = 1, 3$ run over the three species in point, hydrons, electrons and phonons.

This motivates the formulation of a mesoscale-continuum model capable of investigating the consequences of the Keldysh analysis on the scale of the experimental device.

III. The HEP multi-fluid model

In this section we portray a prospective fluctuating-hydrodynamic continuum model of the physical set-up discussed in the previous section. The idea is to import first-principle information from the Keldysh analysis at the level of friction and fluctuating forces, to be inserted in the multi-fluid continuum model.

A. The water fluid

The water fluid obeys the standard continuity plus Stokes equations.

$$\partial_t n_w + \partial_a (n_w u_a) = 0 \quad (1)$$

$$\partial_t (n_w u_a) + \partial_b (n_w u_a u_b + p \delta_{ab} + \sigma_{ab}) = F_a + F_a^h \quad (2)$$

where F_a are bulk forces while F_a^h is the set of applied forces due to interfacial inter actions. Note that, despite the very low Reynolds numbers, we have retained the inertial term, since such term is responsible for important nanoscale

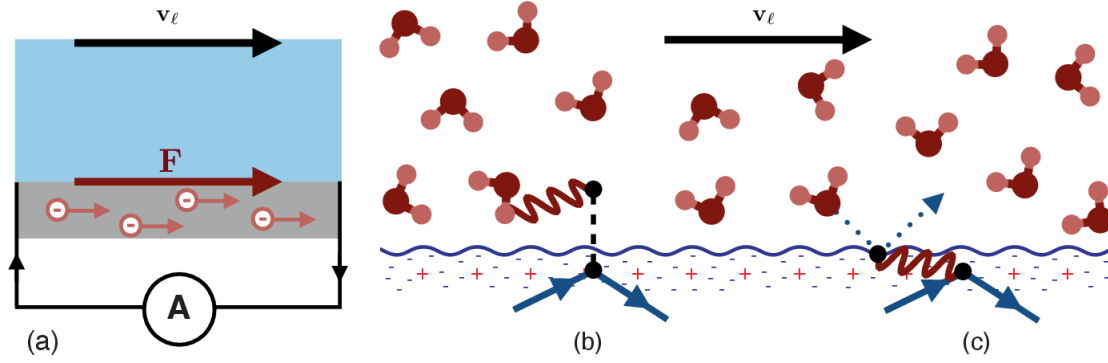


Fig. 2 Electron current-drive scenario. (a) A nanofluidic device whereby liquid water drives an electronic current in the solid, through two related but distinct mechanisms: (b) Hydrons in liquid water impart momentum to the electrons in the solid through Coulomb interactions across the L/S solid interface. (c) Electrons in the solid are driven by phonons excited by water molecule collisions with the solid molecules. From Ref [3].

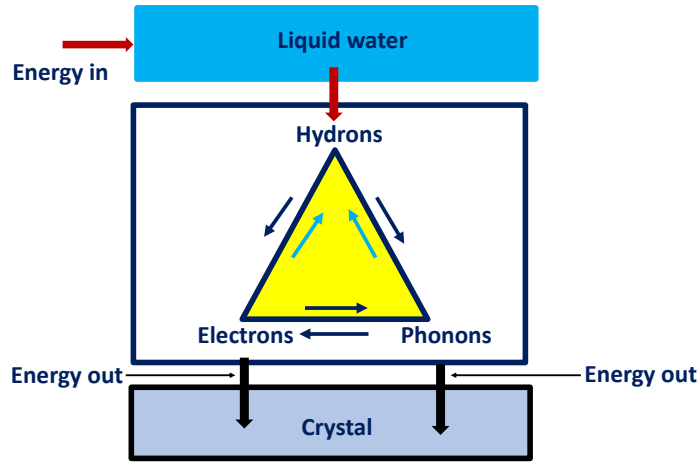


Fig. 3 The energy flow-chart of the HEP multi-fluid model. The water flow (top) is driven by a pressure gradient and dissipates energy at the liquid/solid interface. Dissipation takes places through mutual momentum exchanges between the three "fluid" species, hydrons (H), electrons (E) and phonons (P). These interactions are governed by effective friction coefficients γ_{kl} , $h, l = h, e, p$ which can go both ways depending on the physico-geometrical conditions, primarily on the electron density. The standard energy pathways is downward, hydrons attached to the water molecules receive energy from the pressure gradient and they pass it on to the electrons and phonons in the solid, thus generating a corresponding "phononic" and "electronic" wind. Such winds are stabilized by frictional losses on the crystal atoms, which act as an effective energy sink. The internal pathways are however pretty rich. In particular, when "inverse" couplings (upward flows back to the hydrons) are activated, energy flows back into the hydrons, which is the hallmark of negative quantum friction. Depending on the geometrical and physical parameters such reduction can be pretty substantial, up to fifty percent or more.

hydrodynamic correlations.

B. Hydrons

The hydrons move along with the water fluid, possibly with diffusive effects, hence they obey the continuity-diffusion equation

$$\partial_t n_h + \partial_a (n_h u_a) = D \partial^2 n_h \quad (3)$$

where n_h is the hydron density and u_a is the hydron velocity, which coincides with the velocity of the water fluid. The hydrons influence the motion of the carrier fluid, in which they are immersed, via the body force term F_a^h which embeds four separate contributions: 1) electrostatic contribution due to the interaction of the hydrons with the electrons in the solid, 2) Friction effects due to the interaction with the phonons and electrons in the lattice, 3) Classical fluctuating forces, 4) Quantum fluctuating forces. The electrostatic term it takes the form

$$F^{h,es} = -\nabla (z_h z_e n_h(x) \int V(x, y) n_e(y) dy) \quad (4)$$

where z_h is the hydron charge (both positive or negative depending on whether the charge fluctuations is due mostly to water protons or electrons) and $z_e = -1$ is the electronic charge. In the above $V(x, y)$ is the Debye-screened Coulomb potential. Next, there is the aforementioned frictional drag (vector indices relaxed for simplicity)

$$F^{h,drag} = -m_h \gamma_{he} (u_h - u_e) - m_h \gamma_{hp} (u_h - u_p) \quad (5)$$

where u_e and u_p denote the net velocity of the electron and phonon "fluids" in the solid and m_h is the hydron mass.

Since we are dealing with nanoscale transport, friction must be complemented with fluctuating forces, both thermal and quantum.

According to fluctuating-hydrodynamics, the thermal forces can be expressed as the divergence of the fluctuating momentum flux tensor, as defined by the Fluctuation-Dissipation Theorem:

$$P_{ab}^{cf} = \langle \tilde{F}_a(x_1, t_1) \tilde{F}_b(x_2, t_2) \rangle = \gamma_0 m k_B T \lambda^3 \delta(x_1 - x_2) \delta(t_1 - t_2) \delta_{ab} \quad (6)$$

where γ_0 is the classical collision frequency and $\lambda = v_{th}/\gamma_0$ is the mean free path.

Quantum fluctuations may be treated similarly, but require additional care since, depending on the energy of the quantum excitations, they may involve non-local effects in space and time, depending on their dispersion relation.

$$P_{ab}^{qf} = \langle \tilde{F}_a(x_1, t_1) \tilde{F}_b(x_2, t_2) \rangle = \gamma_0 m k_B T \lambda_q^3 \Gamma_{ab}(x, t; (\frac{x_2 - x_1}{\lambda_q}, \frac{t_2 - t_1}{\tau_q})) \quad (7)$$

In the above, we have defined $x = (x_1 + x_2)/2$, $t = (t_1 + t_2)/2$ and

$$\tau_q = \frac{\hbar}{k_B T} \quad (8)$$

as the typical time scale of thermal quantum fluctuations and $\lambda_q = \hbar/mv_{th}$ as the typical spatial scale (De Broglie length) while Γ_{ab} is the corresponding memory kernel

In the limit $\omega \tau_q \ll 1$ (soft modes), thermal fluctuations prevail and quantum excitations can be treated classically. However, for "hard" quantum fluctuations with $\omega \tau_q > 1$, this is no longer the case. Of course, a realistic estimate of quantum memory effects depends on the specific of the dispersion relation. For instance, hard excitations have usually shorter lifetime than soft ones, hence quantum memory effects are expected mostly from the soft modes. For those modes, the momentum flux tensor may become non-local and the effective force associated with quantum fluctuations can no longer be expressed as the divergence of a one-point tensor.

C. Electron wind in the solid

The treatment is basically the same as for the hydrons, a continuity equation plus a momentum equation supplemented with, i) electrostatic electron-electron and electron-hydron screened Coulomb interactions, ii) friction with phonons and iii) the crystal atom. Fluctuating forces may not needed because the electron orbitals are anchored to the lattice atoms. In equations:

$$F^{es,ee} = -\nabla (n_e(x) \int V_{ee}(x, y) n_e(y) dy) \quad (9)$$

$$F^{es,eh} = -\nabla(n_e(x) \int V_{eh}(x,y)n_h(y)dy) \quad (10)$$

$$F^{fr,eh} = -m_e\gamma_{eh}(u_e - u_h) \quad (11)$$

$$F^{fr,ep} = -m_e\gamma_{ep}(u_e - u_p) \quad (12)$$

$$F^{fr,eC} = -m_e\gamma_{eC}u_e \quad (13)$$

It should be noted that interfacially-driven electrons in the solid move at about half the sound speed of phonons, roughly 1000 m/s, hence they don't require a relativistic treatment as do electronic quasi-particles in graphene [16, 17]. This reflects the fact that the electron wind generated by quantum interfacial effects is very different from electron conduction in graphene (where conduction electrons propagate at about $c/100$). Also to be noted that the water flow is several orders of magnitude slower, typically $u_w \sim 1 \mu\text{s}/m$, reflecting the vast mass separation between the three species in point.

D. Phonon wind in the solid

Likewise, the "phonon fluid" in the solid obeys continuity and momentum equations, the latter supplemented with frictional effects due to phonon scattering with electrons and the crystal atoms. Phonons are linear waves associated with the lattice vibration, their density (occupation number in quantum terms) is proportional to the amplitude of such oscillations and obey a linear-damped wave equation:

$$\partial_{tt}n_p - c_s^2\partial_{xx}n_p = -\gamma_p\partial_t n_p \quad (14)$$

where the frictional force is the sum of phonon-electron and phonon-crystal scattering, namely:

$$F^{fr,pe} = -m_p\gamma_{pe}(u_p - u_e) \quad (15)$$

$$F^{fr,pC} = -m_p\gamma_{pC}u_p \quad (16)$$

$m_p = \hbar k/u_p$ being the effective phonon mass. As a result, $\gamma_p = \gamma_{pC} + \gamma_{pe}(1 - u_e/u_p)$.

IV. The Keldysh Lattice Boltzmann (KLB) implementation

The above fluctuating multi-fluid continuum model could be discretized with grid methods for fluids. In the following we discuss a Lattice Boltzmann implementation [3, 4] on account of the several advantages experienced for the case of microfluidics, and particularly to represent fluid/solid interactions in a way which can seamlessly incorporate microscopic information without taxing computational efficiency. In addition, by using high-order lattices [19], LB can also accommodate classical non-equilibrium effects beyond the realm of continuum mechanics, a statement that holds true also for quantum non-equilibrium transport phenomena. In this respect, the use of novel thread-safe, high-order LB models with reduced memory footprint [20] will be instrumental to efficiently capture the complex non-equilibrium physics of the phenomena at hand without compromising the computational efficiency and scalability of LB models.

Indeed, with the set of fluctuating-hydrodynamic equations discussed in the previous section, the LB implementation can proceed according to well established procedures.

There is a set of discrete distributions for each of the three species involved, say $\{h_i, e_i, p_i\}$ and the corresponding interactions can be encoded according to the standard LB procedures to incorporate external/internal sources. The local equilibria are second order expansions of the flow field of the Bose-Einstein distribution for the bosons (hydrons and phonons) and Fermi-Dirac distribution for the electrons. The implementation of thermal fluctuations is based on the standard fluctuating LB formalism, while quantum fluctuations may require additional care.

Indeed, as it is well known, the classical fluctuating lattice Boltzmann equation incorporates the fluctuating tensor in local form, through the following source term:

$$S_i(x,t) \propto P_{ab}(x,t)w_i(c_{ia}c_{ib} - c_s^2\delta_{ab}) \quad (17)$$

where P_{ab} fulfills the classical FDT relation [14].

In the presence of a two-point quantum-fluctuating tensor $P_{ab}^{qf}(x, x+r; t, t+s)$, the corresponding non-local terms must be implemented. Since this is very expensive, effective one-point closure could be attempted. A possible path

towards this end is to take weighted averages over the the running variables r and s . One could then define a one-point quantum fluctuating tensor as follows:

$$P_{ab}^{qf}(x, t) = \sum_r \sum_s W_x(r) W_t(s) P_{ab}^{qf}(x, r; t, s) \quad (18)$$

with the weight functions suitably patterned after the two-point correlator Γ_{ab} , again an output of the Keldysh analysis.

A. Estimating quantum memory effects

It is useful to inspect some typical orders of magnitude of the main variables at play. The typical quantum thermal frequency is $\omega_q = k_B T / \hbar \sim 40$ ThZ, meaning that the thermal quantum collision time is of the order of 0.1 ps (we remind that $\hbar \sim 6.510^{16}$ eV · sec and $k_B T \sim 1/40$ eV). With a LB timestep of, say, 1 ps, no memory effects need be taken into account since $\Delta t \gg \tau_{qt}$. Hence, the continuum Dirac delta can be safely replaced by its lattice version $\frac{1}{\Delta t}(H(t) - H(t + \Delta t))$, where H denotes the Heaviside step-function. The corresponding quantum thermal energy is about 25 meV, which is comparable with the phonon and electron energies in play, but nonetheless below the energy of the hard modes, which can reach up to a few hundreds meV, namely $\hbar\omega/k_B T \sim 10$. While the details depend on the specific dispersion relation of the quantum excitations, there are reasons to believe that memory effects should be taken into account through informed heuristic relations.

B. Boundary conditions

Since there is flow on both liquid and solid sides of the nanodevice, it seems natural to implement free-slip boundary conditions at the L/S interface for all three species. Denoting by (x_b, y_b) a generic site on the L/S boundary, for each site on the boundary domain we have:

$$h_2(x_b, y_b) = h_4(x_b, y_b + 1) \quad (19)$$

$$h_5(x_b, y_b) = h_7(x_b + 1, y_b + 1) \quad (20)$$

$$h_7(x_b, y_b) = h_5(x_b - 1, y_b + 1) \quad (21)$$

where the discrete speed are numbered according to the standard D2Q9 notation (1=right,2=up,3=left,4=down,5=right-up,6=left-up,7=left-down,8=right-down).

Likewise, for the electrons and the phonons ($f = e, p$), we have:

$$f_4(x_b, y_b) = f_2(x_b, y_b - 1) \quad (22)$$

$$f_7(x_b, y_b) = f_5(x_b - 1, y_b - 1) \quad (23)$$

$$f_8(x_b, y_b) = f_6(x_b + 1, y_b - 1) \quad (24)$$

Once could also possibly implement electron and phonon scattering from the solid atoms via the standard bounce-back no slip boundary conditions, but it is not obvious that this would be an adequate description of such interactions.

At the external upper and lower solid boundaries one can implement no-slip flow, i.e. the bounce back rule, as long as the molecular mean free path remains well below the crossflow direction of the nano-channel. Inlet and outlet boundaries can be handled either by periodic boundary conditions or via Neumann-like boundary conditions as developed in [21], the latter possessing the advantage to be extended to higher-order lattices without any additional algorithmic effort.

V. Prospective applications

As mentioned earlier on, the main scope of KLB is to incorporate genuine non-equilibrium quantum information within a computational harness capable of exploring its effects on a scale of experimental interest. This is of decided interest, because the Keldysh analysis is performed under a number of theoretical restrictions, for instance translational invariance, which are clearly broken when realistic nanodevice geometries are taken in consideration. This is precisely where LB is supposed to bring its added value.

The KLB would allow the quantitative analysis of a number of very interesting applications, centred on the design of quantum-controlled ultra-low friction nanodevices. In particular, one could probe negative quantum friction scenarios at scales of direct experimental relevance. Below, we sketch three prospective possibilities.

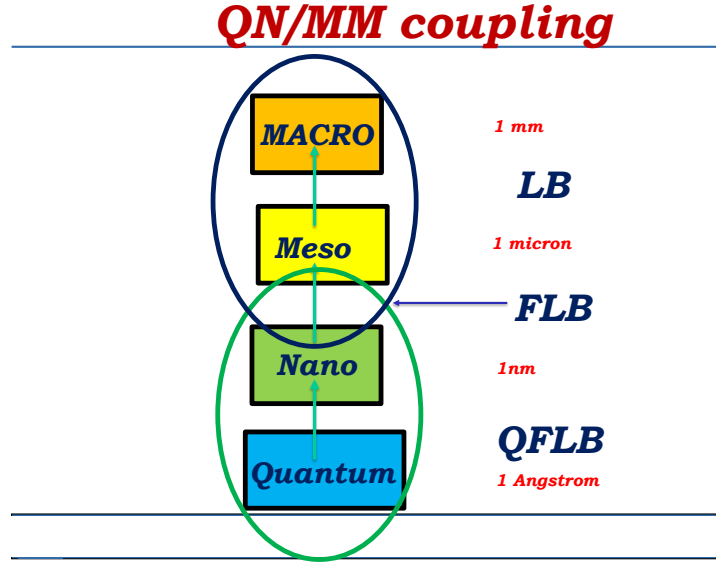


Fig. 4 Schematics of the KLB approach within the multiscale ladder. Lattice Boltzmann was born to address macroscopic fluids, conventionally above 1 mm in the figure and subsequently it was extended to meso-microscale fluids. With the inclusion of fluctuating forces it was brought to nanoscales (FLB). Keldysh Lattice Boltzmann (KLB) goes one level further down, into the quantum non equilibrium realm. This is less surprising than it seems if one considers two "simple" and yet non trivial pieces of evidence. First, at least for simple fluids, the continuum description may hold down to a few nanometers. second, the de Broglie wavelength of thermal electrons in metals is about 10 nm. Hence the quantum and continuum descriptions can definitely shake hands, and the Keldysh Lattice Boltzmann approach just aims at exploiting this overlap.

A. Water permeability in carbon nanotubes

It has been found that the permeability of water scales like the inverse radius of the CNT, a finding which escapes molecular dynamics simulations, indicating that the actual electronic configuration, and not just crystallographic symmetries, dictates nanoscale water transport. Indeed, no such effect is observed with graphite CNT, which share the same crystallographic symmetries of graphene. Likewise, it would of utmost importance to study the effects of nano-corrugations or wrinkles of the graphene sheets on water transport, along the same lines successfully explored by LB simulations of strongly confined microfluids.

The KLB tool could then be applied to the study of water transport in nanotubes, to benchmark against existing treatments and extend the analysis to larger sizes in space and time. The goal is to parametrize quantum friction effects as a function of the design parameters, diameter and length of the nanotube, wall corrugations, and charge carrier density.

B. Droplet-driven graphene currents

Recent experiments have shown that ionic-liquid droplet rolling over graphene sheets can drive substantial electric currents due to the non-equilibrium coupling between droplet charge fluctuations and graphene electrons [5]. The KLB tool could be used to simulate various experimental setups, i.e. varying droplet size and speed and the surface topography to identify the lowest friction scenarios. KLB could enable multi-droplet design, by exploring the effects induced by nonlinear coupling between the electrons in the wake of the first droplet with the charge fluctuations of the second one.

C. Droplet-driven currents in twisted graphene

Electron super-conductivity in magic-angle twisted graphene is one of the most stunning discoveries in modern material science [18]. It is a genuinely electronic effect which is usually tackled by sophisticated electronic structure simulations. However, whenever electrons couple to electro-nano-hydrodynamics, it is legitimate to speculate that new electro-hydro driven electronic effects could arise and be observed via KLB simulations. For instance, it would be

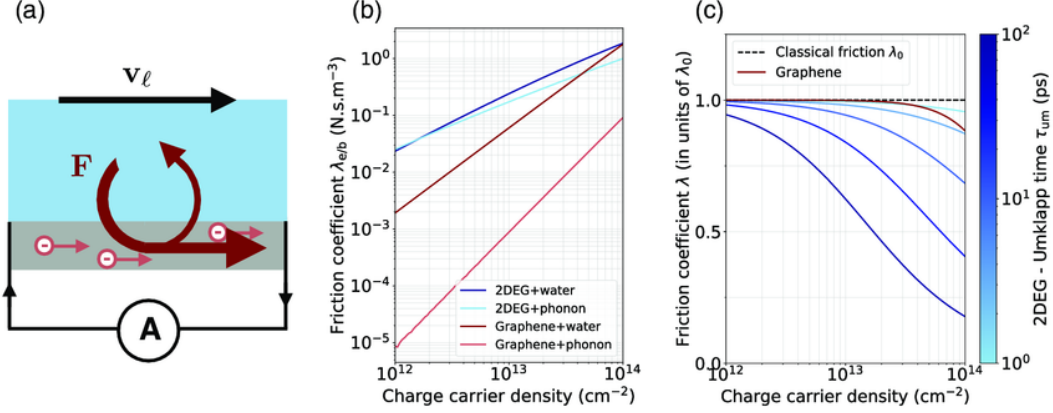


Fig. 5 Negative quantum friction resulting from momentum return from the solid to the liquid via phononic excitations at the liquid/solid interface (from ref. [2].)

interesting to investigate whether non-symmetric flow configurations induced by off-centered charged droplet motions could enhance magic-angle-like effects or perhaps suppress them. This is just one more example of applications that might be pursued via KLB simulations.

VI. Computational feasibility

We conclude with some assessment on the computational feasibility of the KLB scenario.

The natural tool of the trade for computational nanofluidics is Molecular Dynamics [8, 9]. Despite the tremendous progress since its inception, MD still falls short of reaching up to the scale of experimental interest. For instance, a (100, 1000) carbon nanotube (100 nm diameter and 1000 nm length) contains about 300 millions water molecules. With order 10 *Kflops* per molecule and timestep, this makes about 3 trillions *flops/step*: a top-of-the line 30 (effective) *Petaflops/s* supercomputer would complete a single timestep in about 100 microseconds. Ticking at 1 fs (10⁻¹⁵ s) timestep, this supercomputer would evolve the full system over a time span of about 1 microseconds/day. Various sources of inefficiency bring this estimate down to about 10 ÷ 100ns/day, which falls short of meeting engineering design criteria by two orders of magnitude. One way out is the resort to hybrid hydro-molecular dynamics (HMD), whereby MD would be confined to the near-wall region, leaving the bulk to a hydrodynamic solver. This is however still demanding and subject to a series of physical on computational open questions [7]. More importantly, it has been shown that slip flow in CNT is largely underestimated by MD, indicating that standard force-field procedures fall short of describing the actual physics of the water-graphene interactions, pointing to a crucial role of electronic degrees of freedom in the solid. Interestingly, ab-initio MD, besides being even more unpractical computing-wise, would also fall short of capturing the basics of quantum friction because the electrons in the solid are non-adiabatically coupled to charge fluctuations in the liquid.

With a lattice spacing $\Delta x = 1nm$, and a time-step $\Delta t = 1ps$, a nanotube of diameter $D = 100 nm$ and length $L = 10D$ takes $100 \times 100 \times 1000 = 10^7$ grid points, so that a device made of ten such nanotubes side by side would take 100 million points, a modest size for today's LB standards. Extreme LB simulations (hundred billion grid points) can reach thousand times higher, permitting to either increase the resolution or upscale the device by a factor ten along each direction. At a processing speed of 100 *GLUPS*, 100 billion lattice sites are updated every second, hence one million steps (1 microsecond) take roughly 1Ms, about two weeks wall clock time (1000 ns/day, versus 10 ns/day of the current leading edge MD simulations). So much for extreme simulations. Standard KLB could operate with one billion grid points, bringing the wall clock time down to a few hours, which is totally compatible with engineering design requirements [20]. To be noted that KLB operates basically at the same spatial resolution of MD, namely 0.1 ÷ 1 nm, but on a much coarser time-scale. The key point is that, while MD needs timesteps much shorter ($\Delta t/\tau_c \sim 1/100$) than the typical collision time in order to conserve energy, thanks to the exact streaming and built in conservative collisions, LB affords stable operation with timesteps $\Delta t/\tau_c \sim 1$.

This shows that KLB is computationally feasible and may offer a very appealing tool tool to inspire and guide a new generation of experiments suggesting new strategies to design low-friction nanofluidic devices at the quantum level.

VII. Summary

Summarizing, we have sketched a prospective scenario to embed ab-initio non-equilibrium quantum transport effects within a fluctuating continuum hydrodynamic model, to be implemented within a Lattice Boltzmann framework.

The task is intense but seemingly feasible, both conceptually and computationally. As a potential major extension as compared to existing LB schemes we have pointed out the prospect of implementing a non-local version of the fluctuation dissipation theorem for long-memory quantum correlations, both in time and space. The actual manifestation of such non-local effect is very likely to depend on the specific application in point, but in case the need arise, a prospective one-point effective formulation has been briefly discussed. Needless to say, these are simply feasibility considerations, the real test lies within actual simulations, hopefully to be tackled in the near future.

VIII. Acknowledgments

The author is grateful to L. Bocquet for introducing him to the beautiful subject of quantum nanofluidics and for many invaluable insights. This work was triggered by the Symposium "La nanofluidique à la croisée des chemins", College de France, Paris, May 2023.

IX. Appendix: The Keldysh analysis

The Keldysh formalism is based on the dynamic equation for the Green function associated with the particle generation and destruction operators $\hat{\Psi}$ and $\hat{\Psi}^+$

$$G_K(x_1, x_2; t_1, t_2) = \langle [\hat{\Psi}(x_1, t_1) \hat{\Psi}(x_2, t_2)]_- \rangle \quad (25)$$

where subscript $-$ denotes the anticommutator. By setting $X = (x_1 + x_2)/2$, $x = (x_1 - x_2)/2$, $T = (t_1 + t_2)/2$ and $t = (t_2 - t_1)$ and taking the Fourier-transform, we obtain the Keldysh Green function in eight-dimensional phase-spacetime (X, P, E, T)

$$G_K(X, T; P, E) = \int e^{-i(Px - Et)/\hbar} G(x, X; t, T) dx dt \quad (26)$$

Clearly, for the homogeneous case, the dependence on X and T drops out, but since we shall be dealing with quantum non-equilibrium transport phenomena, such an assumption is not justified. The equation for G_K can be derived from first principles, i.e for the underlying Schrodinger equation in second quantized form. Understandably, this is overly complicated, and the fact of living in eight-dimension surely does not help. Nevertheless, in a series of inspiring papers, the authors managed to derive a number of important insights based on analytical manipulations of the Keldysh Green function under the hypothesis of homogeneity.. The main result is that the three species experience a frictional drag linearly proportional to their relative net flow velocity, just like in a classical Langevin framework. The quantum non-equilibrium features remain hidden in the values of the friction coefficients, i.e.

$$F_{kl} = -F_{lk} = \gamma_{k,l}(u_k - u_l) \quad (27)$$

where $k, l = 1, 3$ run over the three "species" h (hydrons), e (electrons) and p (phonons).

References

- [1] Kavokine, N., Netz, R. R., & Bocquet, L. (2021). Fluids at the nanoscale: From continuum to subcontinuum transport. Annual Review of Fluid Mechanics, 53, 377-410.
- [2] Kavokine, N., Bocquet, M. L., & Bocquet, L. (2022). Fluctuation-induced quantum friction in nanoscale water flows. Nature, 602(7895), 84-90.
- [3] Higuera, F. J., Succi, S., & Benzi, R. (1989). Lattice gas dynamics with enhanced collisions. Europhysics letters, 9(4), 345.
- [4] Succi, S. (2018). The lattice Boltzmann equation: for complex states of flowing matter. Oxford university press.
- [5] Coquinot, B., Bocquet, L., & Kavokine, N. (2023). Quantum feedback at the solid-liquid interface: Flow-induced electronic current and its negative contribution to friction. Physical Review X, 13(1), 011019.
- [6] Lizée, M., Marcotte, A., Coquinot, B., Kavokine, N., Sobnath, K., Barraud, C., ... & Siria, A. (2023). Strong electronic winds blowing under liquid flows on carbon surfaces. Physical Review X, 13(1), 011020.

- [7] Delgado-Buscalioni, R., & Coveney, P. V. (2003). Continuum-particle hybrid coupling for mass, momentum, and energy transfers in unsteady fluid flow. *Physical Review E*, 67(4), 046704.
- [8] Werder, T. Walther, J. H., Jaffe R.L., Halicioglu, T. & Komoutsakos, P., (2003). On the water-carbon interaction for use in molecular dynamics simulations of graphite and carbon nanotubes. *The Journal of Physical Chemistry B*, 107(6), 1345-1352.
- [9] Papadopoulou, E., Kim, G. W., Koumoutsakos, P., & Kim, G. (2023). Molecular dynamics analysis of water flow through a multiply connected carbon nanotube channel. *Current Applied Physics*, 45, 64-71.
- [10] Horbach, J., & Succi, S. (2006). Lattice Boltzmann versus molecular dynamics simulation of nanoscale hydrodynamic flows. *Physical review letters*, 96(22), 224503.
- [11] Fyta, M. G., Melchionna, S., Kaxiras, E., & Succi, S. (2006). Multiscale coupling of molecular dynamics and hydrodynamics: application to DNA translocation through a nanopore. *Multiscale Modeling & Simulation*, 5(4), 1156-1173.
- [12] Ladd, A. J. (1994). Numerical simulations of particulate suspensions via a discretized Boltzmann equation. Part 2. Numerical results. *Journal of fluid mechanics*, 271, 311-339.
- [13] Ladd, A. J. (1994). Numerical simulations of particulate suspensions via a discretized Boltzmann equation. Part 2. Numerical results. *Journal of fluid mechanics*, 271, 311-339.
- [14] Dünweg, B., & Ladd, A. J. (2009). Lattice Boltzmann simulations of soft matter systems. *Advanced computer simulation approaches for soft matter sciences III*, 89-166.
- [15] Amadei, C. A., Montessori, A., Kadow, J. P., Succi, S., & Vecitis, C. D. (2017). Role of oxygen functionalities in graphene oxide architectural laminate subnanometer spacing and water transport. *Environmental Science & Technology*, 51(8), 4280-4288.
- [16] Geim, A. K., & Novoselov, K. S. (2007). The rise of graphene. *Nature materials*, 6(3), 183-191.
- [17] Mendoza, M., Herrmann, H. J., & Succi, S. (2013). Hydrodynamic model for conductivity in graphene. *Scientific reports*, 3(1), 1052.
- [18] Cao, Y., Fatemi, V., Fang, S., Watanabe, K., Taniguchi, T., Kaxiras, E., & Jarillo-Herrero, P. (2018). Unconventional superconductivity in magic-angle graphene superlattices. *Nature*, 556(7699), 43-50.
- [19] Montessori, A., Prestininzi, P., La Rocca, M., & Succi, S. (2015). Lattice Boltzmann approach for complex nonequilibrium flows. *Physical Review E*, 92(4), 043308.
- [20] Montessori, A., Lauricella, M., Tiribocchi, A., Durve, M., La Rocca, M., Amati, G., ... & Succi, S. (2023). Thread-safe lattice Boltzmann for high-performance computing on GPUs. *Journal of Computational Science*, 74, 102165.
- [21] Montessori, A., La Rocca, M., Amati, G., Lauricella, M., Tiribocchi, A., & Succi, S. (2024). High-order thread-safe lattice Boltzmann model for HPC turbulent flow simulations. *arXiv preprint arXiv:2401.17074*.